

A Comparative Study of α -Hemolysin Expression in Supported Lipid Bilayers of Synthetic and Enriched Complex Bacterial Lipid

Angélique Coutable · Irina Randrianjatovo · Vincent Noireaux ·
Christophe Vieu · Christophe Thibault · Emmanuelle Trévisiol ·
Jean M. François

© Springer Science+Business Media New York 2014

Abstract The purpose of this short communication was to examine whether the formation of a supported lipid bilayer (SLB) made with purely synthetic lipid or with *Escherichia coli* complex lipid may have any influence on the production and incorporation of the transmembrane protein α -hemolysin from *Staphylococcus*. Different molar ratio of *E. coli* total extract lipid and synthetic 1-palmitoyl-2-oleoyl-*sn*-glycero-3-phosphocholine (POPC) were used to prepare SLB, which were characterized by combination of quartz crystal microbalance with dissipation monitoring (QCM-D), fluorescence recovery after photobleaching (FRAP), and atomic force microscopy (AFM). It was found that a 68:32 molar ratio was

optimal to produce a SLB mimicking a bacterial lipid membrane. Comparing this later SLB with a purely synthetic SLB (100 % POPC) as receptacle for expression of the *Staphylococcus* α -hemolysin fused to eGFP by a cell-free expression system (CFES), we showed that both production and incorporation of this membrane protein was very similar.

Keywords Supported lipid bilayer (SLB) · Biomimetic lipid bilayer · Cell-free transcription-translation · Membrane protein · α -Hemolysin

Electronic supplementary material The online version of this article (doi:10.1007/s12668-014-0127-8) contains supplementary material, which is available to authorized users.

A. Coutable · I. Randrianjatovo · E. Trévisiol · J. M. François
INSA, UPS, INP, LISBP, Université de Toulouse, 135 Avenue de
Rangueil, 31077 Toulouse, France

A. Coutable · I. Randrianjatovo · E. Trévisiol · J. M. François
INRA, UMR792 Ingénierie des Systèmes Biologiques et des
Procédés, 31400 Toulouse, France

A. Coutable · I. Randrianjatovo · E. Trévisiol · J. M. François
CNRS, UMR5504, 31400 Toulouse, France

A. Coutable · C. Vieu · C. Thibault · E. Trévisiol
CNRS; LAAS, 7 Avenue du Colonel Roche, 31400 Toulouse, France

A. Coutable (✉) · C. Vieu · C. Thibault · E. Trévisiol
UPS, INSA, INP, ISAE; UT1, UTM, LAAS, Université de Toulouse,
31400 Toulouse, France
e-mail: acoutabl@laas.fr

V. Noireaux
Physics Department, University of Minnesota, Minneapolis, MN,
USA

1 Introduction

Cell membranes are crucial structural and functional components of all living cells. They are made of a lipid bilayer containing phospholipid of different biochemical structures and present at different percentage [1]. The complexity of cell membrane has stimulated researches for simpler model systems where biophysical and biochemical properties of cell constituents, such as membrane proteins, and interaction with cellular components, can be investigated under controlled conditions. Thus, designing self-assembly of model membranes onto sensor substrates may constitute an important field of research in, e.g., membrane proteins structure-function, and enabling applications in drug discovery, artificial noses, etc. A model that has received considerable attraction is the supported lipid bilayers (SLBs), which can be formed by adsorption and rupture of lipid vesicles (liposomes) onto various different substrates, as pioneered by McConnell et al. [2]. Silicon oxide or titanium oxide were found as the best surfaces for the production of these SLBs because the rupture of the vesicles can take place under near physiological (temperature and pH) conditions [3–6]. The

method of forming SLBs has been investigated in details by many authors using liposomes made of synthetic phospholipid of low complexity in terms of lipid composition [7–9]. More recently, the tethered bilayer lipid membrane (tBLM) has been used as another model in which a space between the surface and the lipid bilayer membrane has been created through a tethering molecule such as polymer cushion, peptide, and protein [10–12]. In both cases, few studies with SLBs or tBLMs that mimicked a biological membrane in terms of lipid compositions are reported [13–16].

The SLBs or tBLMs are well-designed model systems for detailed molecular and functional studies of membrane proteins, which cannot be carried out on whole cells. However, to achieve this goal, the proteins of interest must be obtained and incorporated into the lipid bilayers. To this end, the cell-free expression system (CFES) has emerged as an exquisite method to produce a reasonable amount of a given protein by putting in the system only a plasmid bearing the gene encoding this protein [17, 18]. This technology has been combined with the synthetic lipid vesicles to allow direct incorporation of the produced protein into liposomes [19] or into planar bilayers [20, 21]. A simple and burning question in respect to these artificial systems is to evaluate whether the complexity in terms of lipid composition of lipid bilayers has any effects on the production and insertion of a membrane protein using the CFES. In this short communication, we show that expression and incorporation of the *Staphylococcus* α -hemolysin protein is equivalent between a SLB made of a synthetic lipid and that made of *Escherichia coli* lipid extracts.

2 Materials and Methods

2.1 Materials

Deionized water used in the experiments and for preparing buffer solutions was ultrapure water (PURELAB Ultra) with a resistance of 18.2 M Ω cm. Buffers used in this work (buffer A: HEPES 10 mM, NaCl 150 mM, pH 7.4; buffer B: HEPES 10 mM, NaCl 150 mM, CaCl₂ 2 mM; and buffer C: PBS 10 mM Na₂HPO₄, 137 mM NaCl, 2.7 mM KCl, pH 7.4) were purchased from Sigma-Aldrich. 1-palmitoyl-2-oleoyl-*sn*-glycero-3-phosphocholine (POPC), *E. coli* total lipid extract, and 1-oleoyl-2-{6-[(7-nitro-2-1,3-benzoxadiazol-4-yl)amino]hexanoyl}-*sn*-glycero-3-phosphocholine (NBD-PC) were from Avanti Polar Lipid (Alabaster, AL).

2.2 Vesicle Preparations

The *E. coli* and POPC lipid solutions dissolved in chloroform (10 mg/mL) were mixed in a 100:0, 85:15, 68:32, 0:100 molar ratio (mol %), respectively. The chloroform was removed

under a stream of nitrogen, and subsequently evaporated for at least 3 h in a vacuum desiccator. The phospholipid mixtures were resuspended in buffer B at a final concentration of 1 mg/mL, and then vigorously stirred. These solutions were sonicated (Sonics Materials 500 W) with a Micro-Tip continuously during 20 min at 40 % power and centrifuged 5 min at 16,000 g twice to eliminate titanium nanoparticles. The size of each vesicle preparation was measured by dynamic light scattering (DLS, Malvern Zetasizer ZS, Malvern Instrument Ltd., UK) to have an average diameter with a relative size distribution of 90 \pm 42 nm. The obtained vesicles of different lipid compositions were then diluted in buffer B at a final concentration of 0.1 mg/mL.

2.3 Cell-Free Expression System for Protein Production

The crude extract was prepared with *E. coli* BL21 Rosetta 2 cells according to the procedure described by Shin and Noireaux [17]. The α -hemolysin-eGFP fusion protein (AH-eGFP) was produced under the condition described in [17] from the plasmid Ptar-AH-eGFP that was constructed from pBEST-Luc (Promega Corporation, Madison, WI). It was added to the cell-free system at a final optimized concentration of 5 nM as determined in a previous work [20].

2.4 Quartz Crystal Microbalance with Dissipation Monitoring

Quartz Crystal Microbalance with Dissipation (QCM-D) experiments were performed on a Q-Sense E4 system using the Qsoft software for data acquisition (Q-Sense®, Sweden). Silicon dioxide quartz crystals (QSX-303) were mounted in QCM-D flow chambers (QFM 401). Crystal sensors coated with SiO₂ were cleaned by immersion in a solution of ethanol 99 % at room temperature, intensely rinsed with ultrapure water and then dried under a nitrogen stream. Prior to be mounted in the flow chambers, the sensors were treated with oxygen plasma (Pico μ W UHP, Diener Electronics) at 200 W, 1.5 mbar, for 5 min. For SLB monitoring, QCM-D chambers were first washed with buffer B at room temperature. The liposome composition of interest (0.1 mg/mL, 1 mL per flow chamber) was injected simultaneously in two chambers at a flow rate of 100 μ L/min. After signal stabilization, flow chambers were rinsed with buffer B at 50 μ L/min during 20 min, followed by a 20-min wash with buffer A at 50 μ L/min, and then with buffer C at 50 μ L/min for 20 min. QCM-D chambers were washed extensively with buffer C (50 μ L/min, 20 min), and temperature was brought to 30 °C. The baseline of frequency shift (Δf) and dissipation variation (ΔD) signals was reset to zero before injection of the cell-free extract, 180 μ L per flow chamber, 40 μ L/min, then 20 μ L/min when cell-free reaction arrived in each flow chamber. The cell-free solutions were incubated for 3 h, without flow. After

incubation, the flow chambers were rinsed with PBS buffer (20 $\mu\text{L}/\text{min}$, 20 min; 40 $\mu\text{L}/\text{min}$, 20 min; 80 $\mu\text{L}/\text{min}$, 20 min). The resonant Δf used for data analysis was from the seventh overtone, since, according to the manufacturer, it is less sensitive to crystal mounting conditions. The crystal sensor has a resonance frequency of 5 MHz, giving a starting resonance frequency of 35 MHz at the seventh overtone.

2.5 Fluorescence Recovery After Photobleaching Analysis

The fluorescence recovery after photobleaching (FRAP) technique was used to characterize SLB on freshly cleaned glass surface. The surfaces were activated with oxygen plasma (Pico μW UHP, Diener Electronics) at 200 W, 1.5 mbar for 5 min. Vesicle suspensions including 1 % NBD-PC (fluorescent lipid molecule) were incubated during 30 min on the activated glass surface then washed with buffers B and A. FRAP experiments were performed using a confocal laser scanning inverted microscope (Zeiss LSM 510 NLO), with a 63X water-immersion objective. A laser pulse at the wavelength of 488 nm (power 15 mW) was used to bleach a spot of 40 μm diameter. Images were taken before and at regular intervals with Zeiss LSM software after photobleaching (every 10 s during the first minute, then every minute for 10 min) and processed with Image J freeware. For each image obtained, fluorescence intensity was normalized using the intensity of a reference area and the bleach spot. The diffusion coefficients were calculated using the equation $D=0.224r^2/t_{1/2}$, where $t_{1/2}$ corresponds to half-life of fluorescence recovery and r the radius of the bleach spot [22].

2.6 Atomic Force Microscopy

Atomic force microscopy experiments were performed using a NanoWizard® III (JPK Instrument, Berlin, Germany). Commercial AFM tips with a pyramid-shaped Si_3N_4 cantilever, Au coating on the reflective side of the tips (MLCT-AUHW, Bruker), and a nominal spring constant of 0.01 N/m were used for all AFM measurements. The spring constant of the cantilever was obtained by the thermal noise method [23], and the calibration of the force sensor was obtained by measuring the signal of the photodiode when the AFM tip is approached against a nondeformable hard substrate. The AFM was operated in contact mode applying minimal forces (<0.1 nN) with a frequency of 1–2 Hz. AFM measurements were performed on a mica (Jbg-Metafix, 24 \times 32 mm) surface with a thickness of 0.1 mm cleaved with adhesive tape before experiments. Prior to AFM analyses, the vesicle suspensions were incubated for 30 min on mica surfaces followed by washing with buffer B and then with buffer A.

3 Results and Discussion

3.1 Search for Optimal Conditions to Produce Biomimetic SLBs Using *E. coli* Lipid Extracts

Merz et al. [13] already reported QCM-D adsorption kinetics of *E. coli* total lipid extract liposomes on SiO_2 surface at different CaCl_2 concentration. Contrary to the classical QCM-D trajectories for SLB formation obtained using a synthetic lipid (e.g., POPC) that is characterized by a drastic drop of the resonance Δf corresponding to adsorption of vesicles on the surface, followed by a rapid rise of Δf to about -26 Hz that is due to a rupture and fusion of the vesicles into a planar bilayer, these authors reported that only the first phase was observed with liposomes made from extracted *E. coli* membrane lipid. These results were interpreted as an aggregation of vesicles on the surface with possible formation of partial and nonplanar SLB. Taking into account this previous work, we looked for lipid mixture between POPC and *E. coli* total lipid extract to generate biomimetic SLBs onto a SiO_2 surface (Fig. 1). As expected, the injection in the QCM chamber of a 100 % POPC liposomes resulted in a rapid drop of Δf to -50 to -60 Hz followed after less than 5 min by an immediate rise of the frequency shift to -25 Hz. This latter value that remained constant even after extensive washing is in accordance with the reference value of a typical SLB made on a SiO_2 as shown by other authors using the same methodology [24, 25]. In contrast, upon the injection of a liposomes solution made with 100 % *E. coli* total lipid extract on the SiO_2 surface,

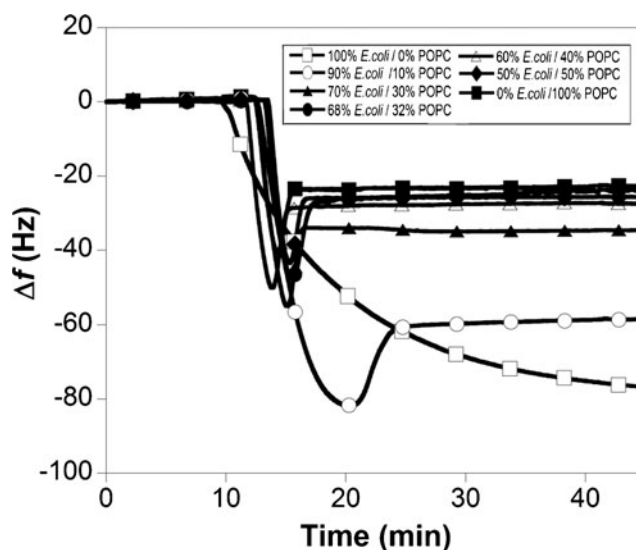


Fig. 1 Quartz crystal microbalance with dissipation (QCM-D) monitoring of the formation of supported lipid bilayer (SLB) onto SiO_2 surface. After stabilization of the baseline level (buffer B), the vesicles (0.1 mg/mL) made with different molar ratio of *E. coli* total lipid extract/POPC were injected in the QCM chambers (10 min). The chambers were washed with HEPES 150 mM, NaCl 10 mM, CaCl_2 2 mM (40 min pour 100:0, 25 min for 90:10, and 18 min for all other composition)

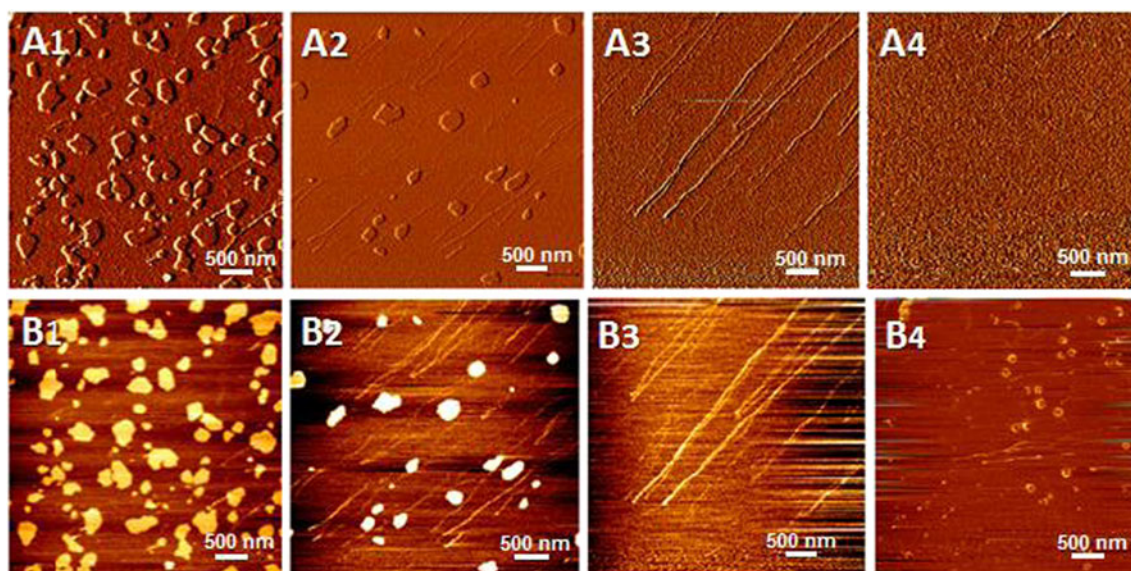


Fig. 2 AFM images ($5\ \mu\text{m}\times 5\ \mu\text{m}$) in contact mode of lipid vesicles incubated onto mica surface prepared from different molar ratio (1) 100 % *E. coli*/0 % POPC, (2) 85 % *E. coli*/15 % POPC, (3) 68 % *E. coli*/32 %

POPC, and (4) 0 % *E. coli*/100 % POPC. **a** Vertical deflection images, **b** height images (color scale, 0–1 nm)

the Δf exhibited a seemingly exponential decrease that was never followed by a resumption of the frequency shift signal. This result suggested the absence of any spontaneous rupture and fusion of the vesicles. From this curve, we could not assess whether a partial supported lipid bilayer has been formed or whether vesicles were adsorbed and aggregated onto the surface. Nevertheless, this result confirmed the previous conclusion of Merz et al. [13] and led us to test mixtures of *E. coli* lipid/POPC at different molar ratio (50:50, 68:32, 70:30, 90:10, 100:0) to produce SLBs. As shown in Fig. 1, the behavior of the QCM-adsorption curve already changed with a molar ratio of *E. coli* lipid/POPC of 90:10, showing after injection a decrease of Δf up to -80 Hz that was followed by a slight rise of this frequency to -60 Hz. This value was about 2.5 times higher than the one expected for a planar bilayer and

thus may indicate the formation of a partial supported lipid bilayer. On the other hand, liposomes solution prepared from a mixture of 50 % *E. coli* lipid/50 % POPC or 68 % *E. coli* lipid/32 % POPC exhibited a QCM-D trajectory very similar to that of 100 % POPC. Altogether, the molar ratio of 68 % *E. coli* extract lipid/32 % POPC was retained as the optimal mixture for producing SLBs that could exhibit biophysical properties closer to *E. coli* cell membranes.

AFM in contact mode was used to image the topology of the adsorbed layers formed from the following four different molar ratios of *E. coli* total lipid extract/POPC: 100:0, 85:15, 68:32, 0:100 on a mica surface previously imaged in buffer solution to check the cleavage quality (see Fig. S1 in supplementary material). As shown in Fig. 2, patches were recorded on a SLB produced with a liposome suspension made of

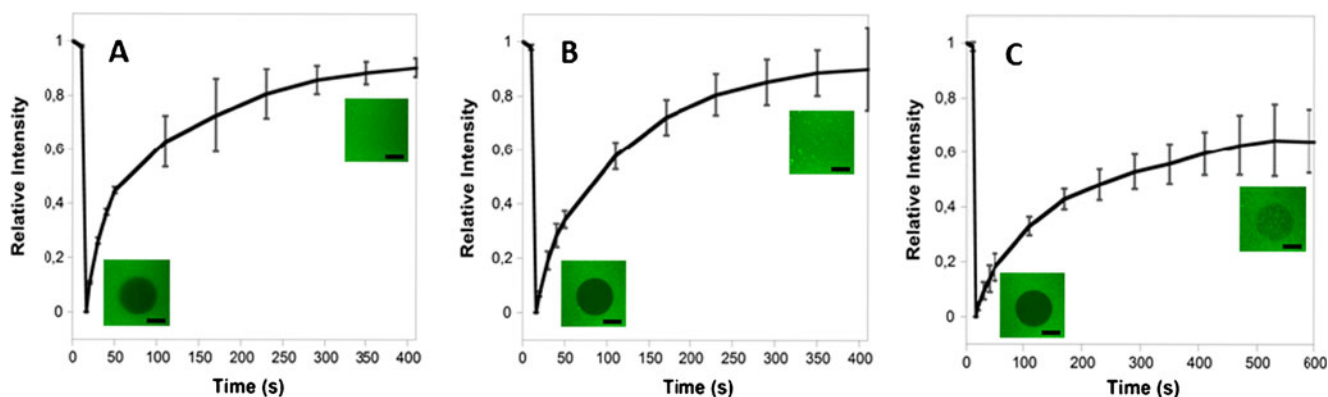


Fig. 3 FRAP data (relative intensity as a function of time and images after photobleaching ($t=0$ min and $t=7$ min), scale bar: $20\ \mu\text{m}$) from a range of different mixture of *E. coli*/POPC/NBD-PC: **a** 0 % *E. coli*/99 %

POPC/1 % NBD-PC, **b** 67.5 % *E. coli*/31.5 % POPC/1 % NBD-PC, and **c** 99 % *E. coli*/0 % POPC/1 % NBD-PC

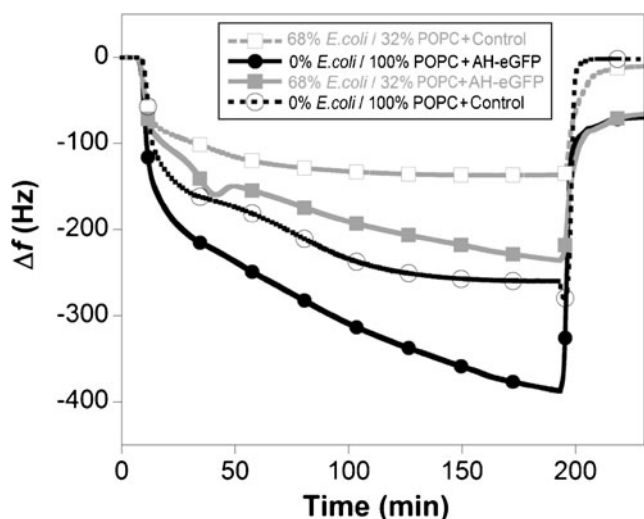


Fig. 4 Quartz crystal microbalance measurement of α -hemolysin-eGFP produced by cell-free expression system on two different SLB (68 % *E. coli*/32 % POPC and 0 % *E. coli*/100 % POPC) at 30 °C. After the baseline level was reset to 0, the cell-free expression system was injected (0 min) and left for 3 h in the QCM chambers, followed by washing with PBS buffer (190 min)

100 % of *E. coli* total lipid extract and of 85:15 molar ratio *E. coli* total lipid extract/POPC. It could be seen that at this molar ratio, the patches formed were less numerous than using 100 % *E. coli* total lipid extract. To explore the nature of these patches, a cross-section profile of AFM images was used to determinate the height of these structures (see Fig. S2 in supplementary material). However, the real height of the lipid patches could not be obtained by contact mode imaging, likely due to strong interactions between the tip and the lipid bilayer [26]. For this reason, we used the tapping mode imaging to show that the height was around 3–4 nm, suggesting that the

observed patches are not segregated domains but real free standing lipid bilayer patches. Conversely, a smooth and regular surface was imaged with liposomes composed of 100 % POPC lipid molecules which was consistent with a planar bilayer membrane structure. AFM images made on surface with liposome suspension composed of a 68:32 molar ratio of *E. coli* total lipid extract/POPC were predominantly the same as those of pure POPC liposomes (Fig. 2), supporting the formation of a correct SLB using this molar ratio.

FRAP technique was a third independent method employed to validate the formation of the “biomimetic” and synthetic SLB. The fluorophore NBD-PC was used to label vesicles made of a molar ratio of *E. coli* total lipid extract/POPC at 100:0, 68:32, and 0:100. These mixtures were incubated for 30 min on glass surface. After flushing away excess of vesicles by extensive wash, FRAP images were recorded before and after photobleaching (Fig. 3) giving rise to normalized recovery curves for the fluorophore as a function of time and for each of the vesicles composition. It can be seen that the recovery kinetic was similar for vesicles made of 100 % POPC and those produced with a mix of 68 % *E. coli* total lipid extract and 32 % POPC, reaching 100 % recovery after 400 s. The calculated coefficient of diffusion was around $1.3 \mu\text{m}^2/\text{s}$ for the former and about $1.0 \mu\text{m}^2/\text{s}$ for the latter condition. In contrast, only 60 % recovery was obtained after 400 s with 100 % *E. coli* extract lipid vesicles, and a calculated coefficient of diffusion of about $0.8 \mu\text{m}^2/\text{s}$. This result is in agreement with a previous report of Dodd et al. [14] that also found a decreased diffusion coefficient between the synthetic SLB and the *E. coli* lipid-based SLB. Taken together, these results obtained with FRAP were consistent with QCM-D measurement and AFM imaging.

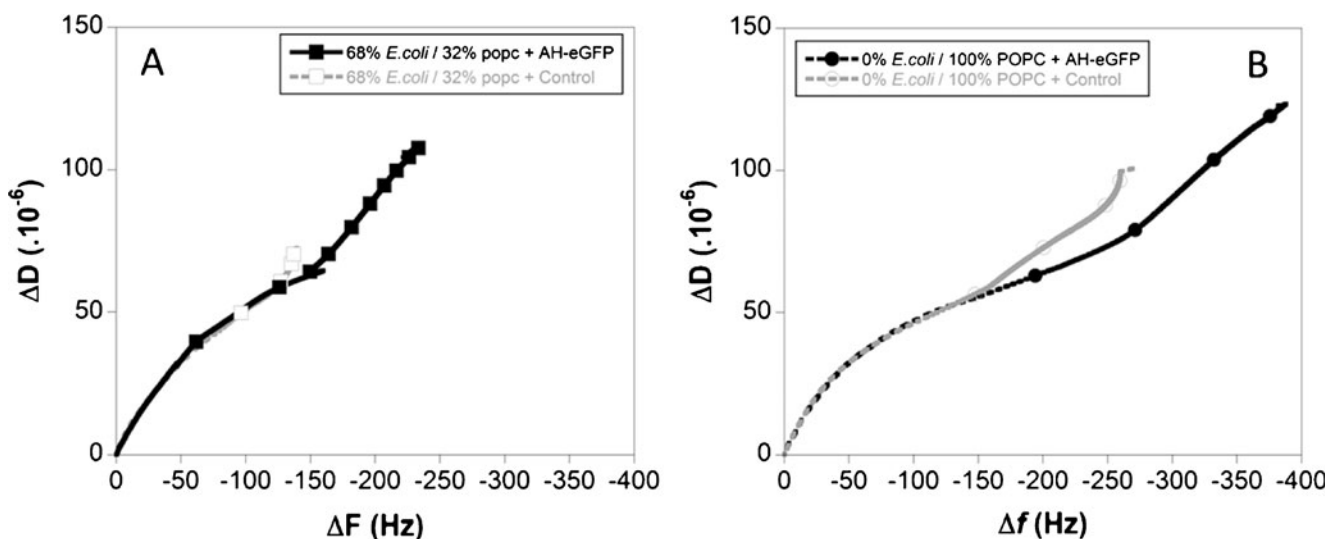


Fig. 5 Dissipation against frequency signal (D-f) of cell-free expression system bearing AH-eGFP (black line) or without plasmid (gray line) on a 68 % *E. coli*/32 % POPC SLB (a) or on a 0 % *E. coli*/100 % POPC SLB (b)

3.2 Cell-Free Production and Incorporation of α -Hemolysin in Synthetic and Bacterial Supported Lipid Membranes

We wanted to compare the production and incorporation of AH-eGFP fusion protein produced by a CFES into SLBs made by synthetic vesicles (e.g., 100 % POPC) and constructed from a 68:32 molar ratio of *E. coli* total lipid extract/POPC, which we considered close to a bacterial lipid membrane (Fig. 4). Cell-free production of the membrane protein was monitored by QCM-D. Since the CFES is enriched of many components needed for transcription and translation machinery that may nonspecifically interact with SLBs, a control experiment without the plasmid bearing the gene encoding AH-eGFP was always performed. After SLBs formation, the baseline of frequency shift was reset to zero before injection of the cell-free expression system into the QCM-D chambers, and the temperature was raised to 30 °C in adequacy with conditions required for optimal working of the CFES [17]. Changes in the seventh overtone resonant frequency were recorded in real time over 4 h after injection in all four QCM-D chambers (two controls without plasmid, the two other with the plasmid). A few minutes after injection, we observed for all conditions an almost instantaneous drop of Δf to approximately -80 to -100 Hz that likely corresponds to unspecific binding of the cell expression components machinery on the SLBs. The frequency shift significantly continued to decrease in the QCM-D chambers containing the CFES with the plasmid to reach -400 Hz for the synthetic SLB (100 % POPC) and to -200 Hz for the SLB made of 68 % *E. coli* total lipid extract/32 % POPC. Since the Δf decreased much less in the control chambers for both types of SLBs, this could indicate that α -hemolysin has been produced by the CFES, which was verified in an independent experiments by a SDS gel electrophoresis (data not shown). After 3 h, all chambers were washed, resulting in a net and rapid reset of the Δf to near the initial baseline level for the synthetic and bacterial lipid mimicking SLBs that were incubated with CFES without plasmid, whereas the value stabilized to -80 Hz with both types of SLBs onto which CFES containing the plasmid has been incubated. This result suggested that a similar amount of AH-eGFP protein was produced and incorporated into the synthetic and the bacterial lipids mimicking SLBs. It was also consistent with aquaporin Z protein produced by a cell-free expression system and inserted into vesicles [17]. Furthermore, if we assume that all the additional mass observed between the experiment and the control condition is attributed to the inserted proteins, than we could estimate the surface density of proteins at the membrane using the Voigt model [27] which gives: 6×10^{12} molecules of α -hemolysin-eGFP for a quartz of 1 cm^2 . However, this mass also includes a huge amount of water molecules. From others studies, we estimate that the proportion of water in this total mass is around 2:3 [28], which finally leads to a molecule

surface density of 2×10^{12} molecules/ cm^2 . The arrangement of the molecules in the membrane is unknown. Assuming that heptamers forming pores are assembled, taking a pore diameter of 8 nm for α -hemolysin pores [29], slightly enlarged to 10 nm due to the eGFP, each heptamer has roughly an area of $8 \times 10^{-13} \text{ cm}^2$. Therefore, 2×10^{12} molecules would represent 3×10^{11} heptamers, which roughly occupies a surface of 0.25 cm^2 ($3 \times 10^{11} \times 8 \times 10^{-13}$). This area is a quarter of the quartz surface, indicating that less than a closed packed monolayer is formed at the sensor surface. The amount of protein could be overestimated due to the presence of CFES residues. Thought quite speculative, this result also showed that AH-eGFP protein are produced and incorporated into a SLB.

The dissipation signal plots against the frequency signal (D-f curve, Fig. 5) indicated a rupture in the linearity of the curve, confirming a change in the mechanical properties of the SLB that is likely due to incorporation of the protein [20]. At the end of the whole process, after final washing, the dissipation signal is much stronger in the case of the AH-eGFP insertion ($\Delta D = 44 \times 10^{-6}$) compared to the control experiment ($\Delta D = 10 \times 10^{-6}$). This suggests again that the expression of AH-eGFP induced a consequent rheological modification of the supported membrane.

4 Conclusions

This short note shows that the lipid composition to produce SLBs does not have any impact in the production and incorporation of the α -hemolysin by a cell-free expression system. However, this conclusion must be dampened by the fact that only one membrane protein has been tested and also because only incorporation has been monitored. It is possible that the lipid composition may be a critical factor for the true biochemical function of the incorporated protein.

Acknowledgments This work was supported by the French National Research Agency (ANR) (FLANAMOVE project). The content of this work is the sole responsibility of the authors. QCM-D experiments and AFM imaging were performed at the "Institut des Technologies Avancées en Sciences du Vivant" (Toulouse, France).

References

1. Spector, A. A., & Yorek, M. A. (1985). Membrane lipid composition and cellular function. *Journal of Lipid Research*, *26*, 1015–1035.
2. Tamm, L. K., & McConnell, H. M. (1985). Supported phospholipid bilayers. *Biophysical Journal*, *47*, 105–113.
3. Cremer, P. S., & Boxer, S. G. (1999). Formation and spreading of lipid bilayers on planar glass supports. *The Journal of Physical Chemistry B*, *103*, 2554–2559.
4. Reimhult, E., Zäch, M., Höök, F., Kasemo, B. (2006). A multitechnique study of liposome adsorption on Au and lipid bilayer formation on SiO_2 . *Langmuir*, *22*, 3313–3319.

5. Reimhult, E., Hook, F., Kasemo, B. (2002). Vesicle adsorption on SiO₂ and TiO₂: dependence on vesicle size. *The Journal of Chemical Physics*, *117*, 7401–7404.
6. Cho, N.-J., & Frank, C. W. (2010). Fabrication of a planar zwitterionic lipid bilayer on titanium oxide. *Langmuir*, *26*, 15706–15710.
7. Rossetti, F. F., Bally, M., Michel, R., Textor, M., Reviakine, I. (2005). Interactions between titanium dioxide and phosphatidyl serine-containing liposomes: formation and patterning of supported phospholipid bilayers on the surface of a medically relevant material. *Langmuir*, *21*, 6443–6450.
8. Rossetti, F. F., Textor, M., Reviakine, I. (2006). Asymmetric distribution of phosphatidyl serine in supported phospholipid bilayers on titanium dioxide. *Langmuir*, *22*, 3467–3473.
9. Richter, R. P., Him, J. L. K., Brisson, A. (2003). Supported lipid membranes. *Materials Today*, *6*, 32–37.
10. Jackman, J., Knoll, W., Cho, N.-J. (2012). Biotechnology applications of tethered lipid bilayer membranes. *Materials*, *5*, 2637–2657.
11. Nedelkovski, V., Schwaighofer, A., Wraight, C. A., Nowak, C., Naumann, R. L. C. (2013). Surface-enhanced infrared absorption spectroscopy (SEIRAS) of light-activated photosynthetic reaction centers from *Rhodobacter sphaeroides* reconstituted in a biomimetic membrane system. *The Journal of Physical Chemistry C*, *117*, 16357–16363.
12. Cabe, I. P. M. (2013). Polymer supported lipid bilayers. *Open Journal of Biophysics*, *03*, 59–69.
13. Merz, C., Knoll, W., Textor, M., Reimhult, E. (2008). Formation of supported bacterial lipid membrane mimics. *Biointerphases*, *3*, FA41.
14. Dodd, C. E., Johnson, B. R. G., Jeuken, L. J. C., Bugg, T. D. H., Bushby, R. J., Evans, S. D. (2008). Native *E. coli* inner membrane incorporation in solid-supported lipid bilayer membranes. *Biointerphases*, *3*, FA59.
15. Jadhav, S. R., Sui, D., Garavito, R. M., Worden, R. M. (2008). Fabrication of highly insulating tethered bilayer lipid membrane using yeast cell membrane fractions for measuring ion channel activity. *Journal of Colloid and Interface Science*, *322*, 465–472.
16. Weiss, S. A., Bushby, R. J., Evans, S. D., Henderson, P. J. F., Jeuken, L. J. C. (2009). Characterization of cytochrome bo3 activity in a native-like surface-tethered membrane. *Biochemical Journal*, *417*, 555.
17. Shin, J., & Noireaux, V. (2010). Efficient cell-free expression with the endogenous *E. coli* RNA polymerase and sigma factor 70. *Journal of Biological Engineering*, *4*, 8.
18. Wu, J., & Swartz, J. (2008). High yield cell-free production of integral membrane proteins without refolding or detergents. *Biochimica et Biophysica Acta (BBA) - Biomembranes*, *1778*, 1237–1250.
19. Hovijitra, N. T., Wu, J. J., Peaker, B., Swartz, J. R. (2009). Cell-free synthesis of functional aquaporin Z in synthetic liposomes. *Biotechnology and Bioengineering*, *104*, 40–49.
20. Chalmeau, J., Monina, N., Shin, J., Vieu, C., Noireaux, V. (2011). [alpha]-Hemolysin pore formation into a supported phospholipid bilayer using cell-free expression. *Biochimica et Biophysica Acta (BBA) - Biomembranes*, *1808*, 271–278.
21. Robelek, R., Lemker, E. S., Wiltshch, B., Kirste, V., Naumann, R., Oesterhelt, D., et al. (2007). Incorporation of in vitro synthesized GPCR into a tethered artificial lipid membrane system. *Angewandte Chemie International Edition*, *46*, 605–608.
22. Soumpasis, D. M. (1983). Theoretical analysis of fluorescence photobleaching recovery experiments. *Biophysical Journal*, *41*, 95–97.
23. Hutter, J. L., & Bechhoefer, J. (1993). Calibration of atomic-force microscope tips. *Review of Scientific Instruments*, *64*, 1868.
24. Keller, C., Glasmästar, K., Zhdanov, V., Kasemo, B. (2000). Formation of supported membranes from vesicles. *Physical Review Letters*, *84*, 5443–5446.
25. Keller, C. A., & Kasemo, B. (1998). Surface specific kinetics of lipid vesicle adsorption measured with a quartz crystal microbalance. *Biophysical Journal*, *75*, 1397–1402.
26. Liang, X., Mao, G., Simon Ng, K. (2004). Probing small unilamellar EggPC vesicles on mica surface by atomic force microscopy. *Colloids and Surfaces B: Biointerfaces*, *34*, 41–51.
27. Voinova, M. V., Rodahl, M., Jonson, M., Kasemo, B. (1999). Viscoelastic acoustic response of layered polymer films at fluid-solid interfaces: continuum mechanics approach. *Physica Scripta*, *59*, 391–396.
28. Glasmästar, K., Larsson, C., Höök, F., Kasemo, B. (2002). Protein adsorption on supported phospholipid bilayers. *Journal of Colloid and Interface Science*, *246*, 40–47.
29. Song, L., Hobaugh, M. R., Shustak, C., Cheley, S., Bayley, H., Gouaux, J. E. (1996). Structure of staphylococcal alpha-hemolysin, a heptameric transmembrane pore. *Science*, *274*, 1859–1865.